Received: 24 October 2022 | Revised: 22 April 2023 | Accepted: 1 June 2023

DOI: 10.1002/cnm.3742

APPLIED RESEARCH

WILEY

Influence of needle design and irrigation depth in the presence of vapor lock: A computational fluid dynamics analysis in human oval roots with apical ramification

G. Loroño[1] | J. M. R. Zaldívar[2] | A. Arias[2] | S. Dorado[3] | J. R. Jimenez-Octavio[4]

[1]Departamento de Endodoncia, Universidad Europea de Madrid, Madrid, Spain

[2]Departamento de Odontología Conservadora, Facultad (Estomatologia II) de Odontología, Universidad Complutense de Madrid, Madrid, Spain

[3]Departamento de Ingeniería Mecánica, Escuela Técnica Superior de Ingeniería-ICAI, Universidad Pontificia Comillas, Madrid, Spain

[4]MOBIOS Lab, Instituto de Investigación Tecnológica, Universidad Pontificia Comillas, Madrid, Spain

Correspondence
J. R. Jimenez-Octavio, Universidad Pontificia Comillas, c/Alberto Aguilera 25, 28015, Madrid, Spain.
Email: joctavio@comillas.edu

Abstract

This paper aims to study the removal of a vapor lock located in the apical ramification of an oval distal root of a human mandibular molar, simulating different needles and irrigation depths with computational fluid dynamic. A geometric reconstruction of the micro-CT of the molar shaped up to a WaveOne Gold Medium instrument was used. A vapor lock located in the apical 2 mm was incorporated. Geometries with positive pressure needles (side-vented [SV], flat or front-vented [FV] and notched [N]) and the EndoVac microcannula (MiC) were created to run the simulations. Irrigation key parameters (flow pattern, irrigant velocity, apical pressure, wall shear stress) and vapor lock removal were compared among the different simulations. Each needle behaved differently that is, FV removed the vapor lock from one ramification and had the highest apical pressure and shear stress values; SV removed the vapor lock in the main root canal but not in the ramification and reached the lowest apical pressure from the positive pressure needles; N was not able to completely remove the vapor lock and showed low apical pressure and shear stress; MiC removed the vapor lock from one ramification, had negative apical pressure and the lowest maximum shear stress. The main conclusion is that none of the needles showed complete removal of vapor lock. MiC, N, and FV were able to partially remove the vapor lock from one out of the three ramifications. However, SV needle was the only simulation that showed high shear stress with low apical pressure.

KEYWORDS

apical delta, computational fluid dynamics, microCT, negative pressure irrigation, positive pressure irrigation, vapor lock

1 | INTRODUCTION

The penetration of irrigants in the full extent of the root canal system is advisable for a complete mechanical and chemical efficacy of endodontic solutions. The main purposes of irrigation are to reduce the microbial load and to eliminate organic tissue and detritus that might be infected.[1–3] Sodium hypochlorite (NaOCl) is currently the most used irrigating

solution due to its tissue-dissolving and antimicrobial properties.[4,5] However, its capacity to reach the whole anatomy of an imbricated root canal system with anatomical irregularities (such as lateral or apical ramifications, isthmuses, and deltas) without risk of extrusion continues being a challenge.[6] Particularly, apical ramifications have been related to endodontic treatment failure when they are large enough to harbor significant numbers of bacteria.[7,8] In fact, 79% of molars have lateral or accessory foramina with diameters ranging from 10 to 200 μm[9]; and more specifically, distal roots of mandibular first molars contain an average of 3.36 portals of exit in the apical 0.5 mm.[10]

Apart from the anatomic irregularities, other factors also affect the capacity of NaOCl to reach the last apical millimeters of the root canal system: the presence of organic tissue or dentinal debris, irrigant properties (such as surface tension, viscosity and density),[11] the delivery mode (irrigant flow rate and needle design),[12–14] the maintenance of apical patency[15] the use of agitation systems (sonic and ultrasonic activation among others),[5,16] the occurrence of procedural errors (e.g. incorrect shaping or ledges), the diameter of the canal instrumentation,[17] and physical phenomena such as vapor lock.[18,19] In fact, the presence of gas bubbles, (the so-called vapor lock) in the apical portion of the root canal blocking the penetration of the irrigant has been an important concern for a decade[18–25] and it is still a challenge.

Vapor lock has classically been attributed to a physical and a chemical phenomenon. Physically, an entrapment of air bubbles occurs when the irrigant is delivered and advances in a dry root canal with a close-end system.[16,24] Chemically, a coalescence of gas bubbles is produced when NaOCl reacts with organic tissue.[16,26] As a result, the irrigating solution is unable to completely reach the internal anatomy jeopardizing the satisfactory cleaning of the complete root canal system.

On one hand, Boutsioukis et al.[19] suggested that vapor lock could be easily prevented or removed with syringe irrigation by increasing the apical size, using open-ended flat needles, positioning the needle closer to working length (WL) and delivering the irrigant at higher flow rates. However, these conclusions were reached in simple artificial geometries and the risk of extrusion was not addressed. On the other hand, when using real anatomies, Tay et al.[18] demonstrated that the presence of vapor lock negatively affected the debridement capacity of the irrigants. Moreover, flat needles were associated to high apical pressure (P_a) values.[13] In fact, irrigation efficacy should be balanced with the risk of extrusion, and to date there is very limited information about P_a values and extrusion risk in the presence of vapor lock.

Several devices have been designed to avoid the extrusion of irrigants to the periapical tissues, among them the EndoVac system (Discus Dental, Culver City, CA). The device includes a microcannula (MiC), that placed at WL allow the penetration of the irrigant up to WL with low risk of extrusion.[27,28] This cannula has demonstrated to be more effective than syringe-needle irrigation and sonic or passive ultrasonic activation reaching the WL.[29] However, the efficacy of syringe-needle irrigation and MiC for removing vapor lock from apical ramifications has not been studied yet.

Computational fluid dynamic (CFD) is a non-invasive validated method to observe the behavior of irrigants and irrigation key magnitudes (wall shear stress (τ_w), flow velocity, irrigant replacement and P_a) in the root canal system.[30–32] It allows the standardization of samples and reduce human errors. Thus, the aim of this study was to analyze the influence of needle design and irrigation depth in the removal of a simulated vapor lock and to assess CFD key irrigation magnitudes during syringe and MiC irrigation in the apical ramification of an oval distal root of a human mandibular molar when a vapor lock is present.

2 | MATERIALS AND METHODS

This study was performed with the approval of the Ethics Committee (CIPI/19/164) and developed based on a previously published model.[14] In brief, the geometric reconstruction (Geomagic 3D Sytems software [Rock Hill, SC, United States]) of a micro-CT (isotropic voxel size of 30 μm/1001 cross-sectional slice images [TIFF format]) of a mandibular molar with an oval distal root canal with an apical ramification was used. The root canal was shaped up to a WaveOne Gold Medium instrument (nominal size #35/ taper 0.06*v*; Dentsply Sirona endodontics, Ballaigues, Switzerland), but the instrument only entered the first branch of the ramification.

Four different types of needles were used in the study, two closed-ended and two open-ended. The two closed-ended needles were a side-vented needle (SV) and multivented (EndoVac Microcannula [MiC]). The two open-ended needles were flat or front-vented (FV) and notched needle (N). The geometry of SV, FV and N was modeled following international standard ISO 9626:2016 specifications for irrigation needles with an external diameter of 0.30 mm and internal diameter of 0.19 mm. The SV was modeled reproducing the geometry of the Max-i-Probe needle (Dentsply/Tulsa Dental, York, PA, USA) which is designed with a 0.5 mm side-vent located 1 mm from the tip. The N needle was modeled as a Monoject needle (Covidien, Dublin, Ireland) with a notch-vent of 2.5 mm in the latest millimeters. The design of the MiC was based in previous studies.[27] Different geometries were created with each positive pressure needle (SV1,

SV3, FV1, FV3, N1, N3); two different irrigation positions, 1 and 3 mm from WL, were chosen for each of them due to the influence of needle working length on irrigation results[32]; and the MiC placed at WL following manufacturer's direction for use.

The main difference with the previous study[14] was the incorporation of a vapor lock located in the apical 2 mm of a real root canal with an apical ramification, see Figure 1. The spatial discretization of the fluid domain was performed with ANSYS 18.2 (Fluent Inc., Lebanon, NH, USA). A two-phase flow (gas and liquid) was represented in the root canal. The gas, ambient air, in the apical 2 mm simulated the vapor lock and the liquid simulated the irrigant in the rest of the root canal.

A summary of the characteristics related to the material properties, boundary conditions and numerical modeling are detailed in Table 1. The numerical simulation was run with the CFD extension of ANSYS 18.2 (ANSYS Fluent, Canonsburg, PA, USA).

The k-ω shear stress transport (SST) turbulence model is a popular two-equation model used for predicting turbulent flows first presented by Menter.[33] It combines the benefits of both the k-epsilon and k-omega models, overcoming their limitations in different regions of the flow. The model uses the turbulence kinetic energy (k) and the specific dissipation rate (ω) as primary variables. The k equation models the transport of turbulent kinetic energy and its dissipation (Equation 1), while the ω equation models the transport of the specific dissipation rate (Equation 2). The model employs two different formulations for the turbulent viscosity in the near-wall and outer regions. In the near-wall region, it reduces to a low-Reynolds number version of the k-omega model, while in the outer region, it behaves like the k-epsilon model.

The k-w SST model equations are as follows:

$$\partial(\rho k)/\partial t + \partial/(\partial x\_i)\,(\rho k U\_i) = P\_k - \beta^{*}\,\rho\omega k + \partial/(\partial x\_j)\,[(\mu + \mu\_t\,\sigma\_k)\,\partial k/(\partial x\_j)], \tag{1}$$

$$\partial(\rho\omega)/\partial t + \partial/(\partial x\_i)\,(\rho\omega U\_i) = (\gamma P\_k)/\nu\_t - \beta\rho\omega^{2} + \partial/(\partial x\_j)\,[(\mu + \mu\_t\,\sigma\_\omega)\,\partial\omega/(\partial x\_j)], \tag{2}$$

where k is the turbulence kinetic energy, ω is the specific dissipation rate, u is the velocity vector, Pk is the production of turbulence kinetic energy, β and β^{*} are empirical constants, γ is a constant, νt is the turbulent viscosity, μ is the molecular viscosity, and ρk and $\rho\omega$ are blending functions that switch between the k-epsilon and k-omega models.

Overall, the k-ω SST turbulence model is widely applicable in many engineering fields and has been extensively validated against experimental data.

A two-phase model simulation was used to study a complex fluid system in a CFD study. The Volume of Fluid (VOF) method with an explicit formulation was employed to capture the interface between the two phases. The volume fraction cutoff was set to 1e−6, and a Courant number of 0.25 was used for numerical stability. This allowed for accurate tracking of the fluid–fluid interface and provided valuable insight into the dynamic behavior of the fluid system.

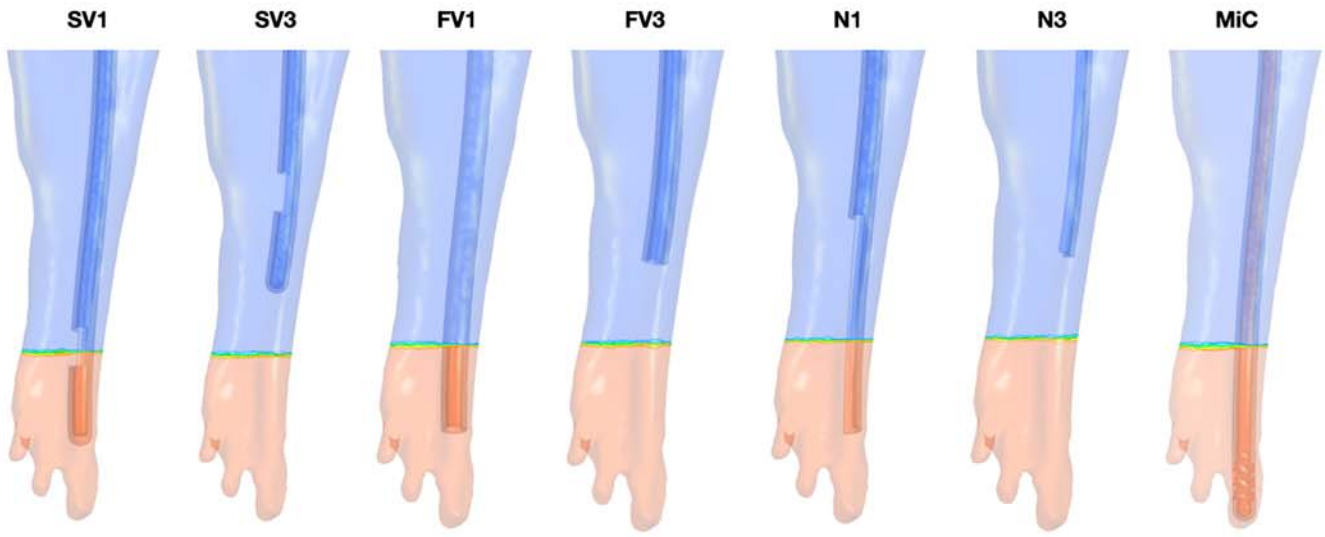

FIGURE 1 CAD models for all simulations. Notice the two-phase flow represented in the root canal: ambient air in the apical 2 mm representing the vapor lock and liquid representing the irrigant in the rest of the root canal.

TABLE 1 Summary of characteristics related to the material properties, boundary conditions and numerical modeling.

	Item	Property	Value	Description
Material properties	Irrigant	Density	998.0 kg/m^3	Incompressible, Newtonian, homogeneous, isothermal and immiscible
		Viscosity	0.986×10^{-3} Pa s	
	Vapor lock	Density	1.135 kg/m^3	
		Viscosity	1.920×10^{-5} Pa s	
Boundary conditions	Canal walls			Rigid, impermeable and flat
	Irrigation elements			Rigid, impermeable and flat
	Inlet	Velocity	0.1 g/s	6 mL/min in corono-apical direction
	Outlet	Pressure	857.5 mmHg	Atmospheric pressure in the coronal access
		Pressure	97.5 mmHg	Aspiration power of the MiC
	Gravity	Acceleration	9.8 m/s^2	
Numerical modeling	Flow	Type		Transient
	Turbulence	Model		k-Ω SST
		Backflow intensity	5%	
		Viscosity ratio	10.0	
	Time	Step	10^{-3} s	
		Simulation	0.6 s	
	Software			ANSYS 18.2 (ANSYS Fluent, Canonsburg, PA, USA)
	Hardware			Dell Intel Xeon® (CPU ES 2680 0 2 × 2.70 GHz, 32 GB RAM memory and a 64 Bits operative system) server

ANSYS FLUENT Meshing module was used to obtain the mesh for this model. Three different areas were defined for different mesh sizes. The volume close to the apex and constituting the needle flow had elements with a size 0.06 mm. The middle third of the tooth has elements with a size of 0.1 mm. The upper third had elements with a size of 7 mm. These sizes were decided along with the relevancy of the potential results. Main interest will be found at the apex; therefore, a more precise mesh is needed in that volume. Convergence tests were conducted on the mesh, which demonstrated that the solution was stable and accurate with respect to the mesh resolution.

Irrigation magnitudes (flow behavior and velocity, τ_w distribution and P_a values) were evaluated and compared among the simulations. Furthermore, P_a from each simulation was compared against a 25-mmHg threshold[14] in order to prevent sodium hypochlorite accident, whilst τ_w was compared against a 0.75-mmHg threshold[34,35] as likely minimum shear stress for efficient debriding. Streamlines and velocity maps were also calculated and compared.

3 | RESULTS

Each specific needle and the Mic behaved differently in the presence of vapor lock. Figure 2 illustrates streamlines, velocities, τ_w values, canal pressures and presence of vapor lock for all simulations; and Figure 3 shows maximum τ_w (A) and maximum P_a values for each simulation (B).

3.1 | Side-vented needle

In general, the behavior of SV needle in removing the vapor lock varied when tested at 3 or 1 mm from WL. It also showed the lowest maximum P_a values from the three positive pressure needles tested. τ_w values higher than 1 mmHg were located in a small area near the needle outlet (Figure 2).

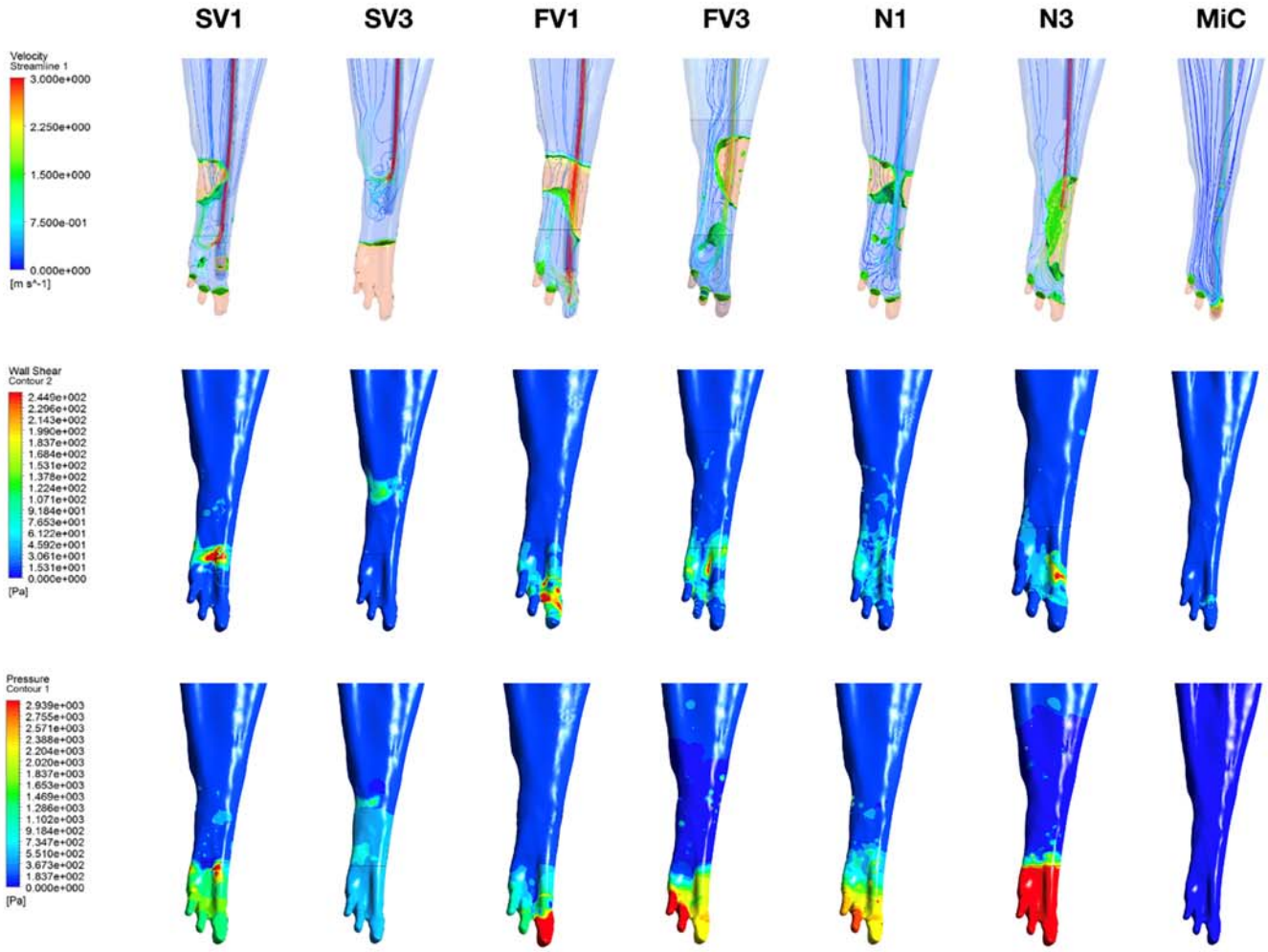

FIGURE 2 Streamlines of velocity (top), shear stress (middle) and canal pressure (down) after all simulations.

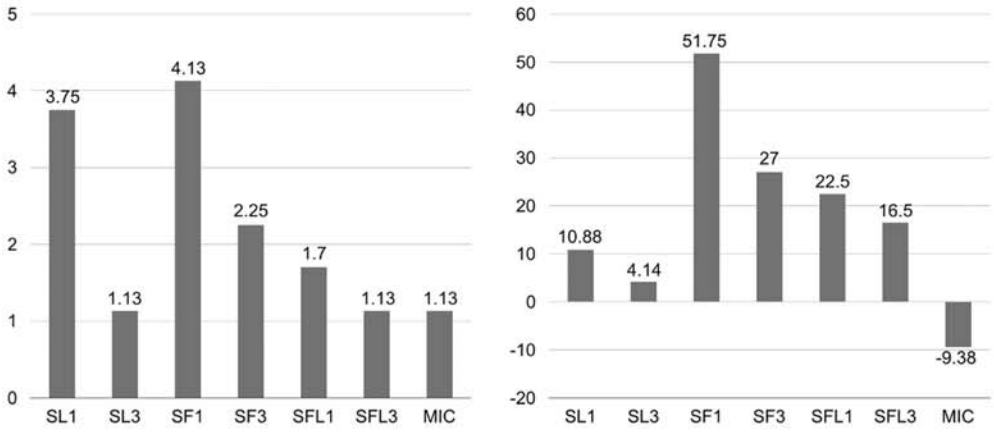

FIGURE 3 Maximum shear stress [mmHg] (left) and Maximum apical pressure [mmHg] (right) values for each simulation.

Simulation SV3 showed a practically intact vapor lock and low velocities, P_a (4.1 mmHg) and τ_w (1.1 mmHg). On the contrary, SV1 removed the vapor lock in the main root canal, although not in the ramifications. At the same time, it displayed higher P_a, velocity and τ_w values. P_a values were still far from the threshold for risk of extrusion (10.9 mmHg) and τ_w values were the second highest for all needles (3.7 mmHg).

3.2 | Flat or front-vented needle

In general, FV needle showed high τ_w and P_a values and it was not able to completely remove the vapor lock.

Simulation FV3 showed a slight penetration of irrigant into one of the three ramifications, P_a values slightly above the risk of extrusion threshold (27 mmHg) and relatively high maximum τ_w (2.3 mmHg). Furthermore, the area showing τ_w values higher than 1 mm Hg was much larger than in SV simulations. However, velocity fluid flow was only high in the main root canal and not inside the ramification.

FV1 was able to remove the vapor lock from one of the ramifications and showed the highest τ_w value (4.1 mmHg). Furthermore, it was able to generate a high velocity fluid flow in the ramification. However, the area with τ_w values higher than 1 mm Hg was significantly lower than in FV3. At the same time, this simulation showed the highest P_a values, far above the threshold considered for risk of extrusion (51.8 mmHg).

3.3 | Notched needle

N needle results were similar independently of the penetration depth. On the one hand, the insertion at 3 mm from WL did not remove the vapor lock from any of the ramifications, had low τ_w values (1.1 mmHg) and very little flow with medium velocities, although maximum P_a values were below the threshold (16.5 mmHg). On the other hand, N1 was not able to remove the vapor lock but had higher maximum τ_w values (1.7 mmHg) when compared to N3. Additionally, it generated low velocities in the main canal, but P_a was also below the risk of extrusion threshold (22.5 mmHg).

3.4 | EndoVac microcannula

MiC removed the vapor lock partially from one of the ramifications; however, it had negative P_a (−9.4 mmHg). At the same time, this simulation displayed the lowest τ_w (followed by SV3 [1.1 mmHg] with simulation N3 [1.3 mmHg]), and low velocities.

4 | DISCUSSION

This study was designed to better understand the fluid dynamics behavior in the presence of vapor lock in an oval root canal anatomy with apical irregularities. The removal of a vapor lock has been previously investigated either with methodologies that could not analyze the fluid parameters[23] or with similar methodologies to the one used in the present study but in artificial and simple geometries.[19] The use of CFD has been previously validated both in the presence[19] and absence of vapor lock.[30] Furthermore, the micro-CT of a human mandibular molar has been used to reproduce fluid dynamics in real anatomies and hence, to better extrapolate the findings to a real clinical situation. As previously reported, mandibular molars commonly have three portals of exit,[10] and the presence of apical ramifications might interfere with the removal of vapor lock in comparison to regular root canals. The upward buoyant force exerted by the vapor lock, which mainly depends on the cross section of the canal ($\approx \pi r^2$), is counteracted by the surface tension that varies with the perimeter of the cross section ($\approx 2\pi r$).[35] This makes easier to remove a vapor lock from wide and regular geometries. This aspect is relevant because the presence of vapor lock in all or part of an apical irregularity may prevent its cleaning[18] and therefore may trigger the failure of a root canal treatment.[7,8]

Boutsioukis et al.[19] analyzed the formation and removal of apical vapor lock with syringe irrigation in a combined in vitro and CFD study. The present study tried to further add information about magnitude parameters like τ_w and P_a, to further understand the effectiveness and safety of irrigation devices when removing a vapor lock. Although the P_a needed to generate an irrigation accident with NaOCl is unknown and subject to clinical variations[36] the threshold used in the present report was determined considering the following three parameters: blood pressure in the intraosseous space (30 mmHg), capillary bed (close to 25 mmHg) and interstitial pressure values (20–30 mmHg).[37] This allows the interpretation of results based on clinically realistic criteria and fear comparisons among simulations. On the other hand, an effort has been made to compare the τ_w among simulations, due to the τ_w needed for the removal of detritus or biofilms adhered to dentine would be sufficient in all the cases according to the threshold reported in the literature.[35,36] Nonetheless, results should be interpreted with caution.

The design of the vapor lock is based on previous studies,[19] simulating an adverse clinical situation in which the most apical 2 mm of the canal presented an air lock. Likewise, the parameters used for the physical properties for both the vapor lock and the irrigant are also based in previous studies.[1,13,19] Furthermore, a turbulent flow was assumed based on Gao et al. and Rito Pereira.[30,38] The irrigation velocity used is clinically realistic[39] and widely described.[14,38] The use of higher velocities might be a future field of study for CFD; although based on the P_a values obtained in the present work it seems reasonable to anticipate that higher velocities may be dangerous for the use of both FV and N needles.

Three commonly used positive pressure needles and a negative pressure device have been analyzed in the present study although some other parameters such as the needle outlet direction has not been evaluated. Wang et al.[40] analyzed the influence of SV needle orientation in the τ_w and P_a produced inside the root canal. In this study, SV needle was oriented in opposite direction to the closest wall. Considering previous results,[40] higher values would have probably been obtained if the needle was oriented differently. However, the results obtained in both studies combined suggest that P_a and τ_w values are noticeably influenced by the type of needle and insertion depth and not by the orientation of the needle outlet. Moreover, two different penetration depths were analyzed in the present simulations to overcome the computational difficulty of analyzing vertical movements of needles when using two-phase flow (air and fluid) in real anatomies. Considering that the maximum values of τ_w and P_a were obtained in the first tenth of a second of the simulation (data not shown), the results probably will not vary greatly if the needle moves vertically. Although Hu et al.[41] recently demonstrated that fluid flow is affected by the movement of the needle inducing lower velocity and P_a than static needles; it must be considered that the use of regular geometries for the purpose may overvalue fluid velocity and P_a through hindering of the backflow compared to real anatomies with oval canals and irregularities that may facilitate the fluid return. In fact, P_a values found in the present study are close to those using different[42] or similar[40] methodologies but real anatomies, and far from those using regular cones.[12,13,41,43]

To date no study has evaluated the effectiveness of the EndoVac system in the removal of vapor lock. It could be assumed that it is a suitable device for its removal based on the mechanism of action; however, the presence of the ramification hindered the removal of the vapor lock and it was only able to partially eliminate it from the ramification in which the MiC entered. In addition, τ_w values with the EndoVac were the lowest when compared to the rest of the simulations. The lowest values were also obtained in a previous study when a vapor lock was not present.[14] The presence of the vapor lock increased the τ_w, but EndoVac still showed identical values to SV3. As expected, a negative P_a was obtained with EndoVac. The P_a obtained in this simulation was even lower than in the absence of a vapor lock (−9.4 mmHg vs. −3.4 mmHg obtained in the previous study) due to the physical properties of the mixture of the two different phases (liquid–gas) above the apical constriction. Bernoulli's principle (which depends on the density ρ and specific weight γ of the fluid, velocity V and pressure P, the acceleration of gravity g and elevation of the point above a reference plane z) states that the equation $\left[\frac{\rho V^2}{2g}+\frac{P}{\gamma}+z\right]$[44] is constant; therefore if the density of air is lower than that of NaOCl, static pressure $\left[\frac{P}{\gamma}+z\right]$ is reduced and hence, dynamic pressure $\left[\frac{\rho V^2}{2g}\right]$ increased. Consequently, the increase of velocity results into higher τ_w and lower P_a values. For this basic physic principle, a bi-phase flow is more efficiently absorbed by the MiC than the irrigant alone (monophase). Furthermore, positive pressure needle simulations presented similar or higher P_a and τ_w values in the presence of vapor lock when compared to those without vapor lock[14] based on the same Bernoulli's principle. At the same time, streamlines also differed considerably in the presence of vapor lock with the most pronounced differences detected when SV needle was placed at 3 mm from WL. Streamlines reached the apical ramification in the absence of vapor lock,[14] but the irrigant flow only reached 0.3 mm apically in the presence of vapor lock and maintained it completely. Similarly, in absence of vapor lock, streamlines showed that FV1 simulation penetrated in two out of the three ramifications, while when vapor lock was present only one ramification was reached and hence vapor lock was only eliminated from this ramification.

It is interesting to notice that none of the needles were able to completely remove the vapor lock from the three ramifications. Moreover, one only simulation removed completely the vapor lock from one ramification (FV1). In terms of vapor lock removal efficacy, SV needle demonstrated the poorest results; although SV1 was able to remove the vapor lock from the main canal and presented the second highest τ_w and low risk of extrusion. At the same time, both N and FV needles presented high risk of extrusion at 1 mm from WL and were not able to remove the vapor lock when situated at 3 mm from WL generating P_a values higher than the SV needle. This result differed from those reported by Boutsioukis et al.,[19] who found high vapor lock removal efficacy with delivery velocities ranging from 5 to 10 mL/min specially in simulated root canals with nominal apical size #50 and 0.04 taper preparations. The difference is very likely due to the anatomical irregularities of real root canals that were not present in previous studies.

Since none of the positive pressure needles were able to remove vapor lock in an apical ramification while avoiding the risk of extrusion; alternative techniques or devices, such as sonic or passive ultrasonic irrigation, must be evaluated in the future in search of a safe and effective irrigation method in the presence of vapor lock. In fact, clinical studies have shown that maintaining apical patency minimized the presence of gas bubbles in big canals.[23] From a practical perspective, neither N nor SV were able to remove the vapor lock from the apical ramification, and FV had P_a values above the threshold determined for risk of extrusion. Moreover, MiC seemed to be the only needle partially effective in terms of vapor lock removal below this threshold, but its cleaning capacity might be compromised due to the low velocity and τ_w. Thus, the combination of SV1 (due to the high maximum τ_w) and MiC might be a suitable clinical approach for the purpose.

Under the conditions of this study, the following can be concluded:

1. None of the needles were able to completely remove the vapor lock.
2. The microcannula and front-vended needle when placed at 1 mm from the working length were able to remove the vapor lock from one of three ramifications, while side-vented and notched needles removed it from the main canal.
3. Front-vented and notched needles obtained apical pressure values above the threshold of extrusion in the presence of vapor lock.
4. Front-vended and side-vended needles placed 1 mm from the working length presented the highest shear stress values.

ACKNOWLEDGEMENTS

The authors deny any conflict of interests related to this study. This research did not receive any specific grant from funding agencies in the public, commercial, or not-for-profit sectors.

CONFLICT OF INTEREST STATEMENT

The authors declare no conflict of interest.

DATA AVAILABILITY STATEMENT

Data sharing not applicable to this article as no datasets were generated or analysed during the current study.

ORCID

A. Arias https://orcid.org/0000-0003-2270-8096
S. Dorado https://orcid.org/0000-0001-9927-6872
J. R. Jimenez-Octavio https://orcid.org/0000-0002-6869-8332

REFERENCES

1. Sjogren U, Hagglund B, Sundqvist G, Wing K. Factors affecting the long-term results of endodontic treatment. *J Endod*. 1990;16:498-504.
2. Lee SJ, Wu MK, Wesselink PR. The effectiveness of syringe irrigation and ultrasonics to remove debris from simulated irregularities within prepared root canal walls. *Int Endod J*. 2004;37:672-678.
3. Haapasalo M, Endal U, Zandi H, Coil JM. Eradication of endodontic infection by instrumentation and irrigation solutions. *Endod Top*. 2005;10:77-102.
4. Conde AJ, Estevez R, Lorono G, et al. Effect of sonic and ultrasonic activation on organic tissue dissolution from simulated grooves in root canals using sodium hypochlorite and EDTA. *Int Endod J*. 2017;50:976-982.
5. Boutsioukis C, Arias-Moliz MT. Present status and future directions—irrigants and irrigation methods. *Int Endod J*. 2022;55:588-612.
6. Robberecht L, Delattre J, Meire M. Isthmus morphology influences debridement efficacy of activated irrigation: a laboratory study involving biofilm mimicking hydrogel removal and high-speed imaging. *Int Endod J*. 2023;56:118-127.
7. Ricucci D, Siqueira JF Jr. Fate of the tissue in lateral canals and apical ramifications in response to pathologic conditions and treatment procedures. *J Endod*. 2010;36:1-15.
8. Ricucci D, Siqueira JF Jr. Anatomic and microbiologic challenges to achieving success with endodontic treatment: a case report. *J Endod*. 2008;34:1249-1254.
9. Dammaschke T, Witt M, Ott K, Schafer E. Scanning electron microscopic investigation of incidence, location, and size of accessory foramina in primary and permanent molars. *Quintessence Int*. 2004;35:699-705.
10. Harris SP, Bowles WR, Fok A, McClanahan SB. An anatomic investigation of the mandibular first molar using micro-computed tomography. *J Endod*. 2013;39:1374-1378.

11. Estevez R, Conde AJ, Valencia de Pablo O, de la Torre F, Rossi-Fedele G, Cisneros R. Effect of passive ultrasonic activation on organic tissue dissolution from simulated grooves in root canals using sodium hypochlorite with or without surfactants and EDTA. *J Endod*. 2017;43:1161-1165.
12. Boutsioukis C, Lambrianidis T, Kastrinakis E. Irrigant flow within a prepared root canal using various flow rates: a computational fluid dynamics study. *Int Endod J*. 2009;42:144-155.
13. Boutsioukis C, Verhaagen B, Versluis M, Kastrinakis E, Wesselink PR, van der Sluis LWM. Evaluation of irrigant flow in the root canal using different needle types by an unsteady computational fluid dynamics model. *J Endod*. 2010;36:875-879.
14. Loroño G, Zaldívar JR, Arias A, Dorado S, Cisneros R, Jimenez-Octavio JR. Positive and negative pressure irrigation in oval root canals with apical ramifications: a computational fluid dynamics evaluation in micro-CT scanned real teeth. *Int Endod J*. 2020;53:671-679.
15. Vera J, Arias A, Romero M. Effect of maintaining apical patency on irrigant penetration into the apical third of root canals when using passive ultrasonic irrigation: an in vivo study. *J Endod*. 2011;37:1276-1278.
16. Gu LS, Kim JR, Ling J, Choi KK, Pashley DH, Tay FR. Review of contemporary irrigant agitation techniques and devices. *J Endod*. 2009; 35:791-804.
17. Boutsioukis C, Nova PG. Syringe irrigation in minimally-shaped root canals using three endodontic needles: a computational fluid dynamics study. *J Endod*. 2021;47(9):1487-1495.
18. Tay FR, Gu LS, Schoeffel GJ, et al. Effect of vapor lock on root canal debridement by using a side-vented needle for positive-pressure irrigant delivery. *J Endod*. 2010;36:745-750.
19. Boutsioukis C, Kastrinakis E, Lambrianidis T, Verhaagen B, Versluis M, van der Sluis LWM. Formation and removal of apical vapor lock during syringe irrigation: a combined experimental and computational fluid dynamics approach. *Int Endod J*. 2014;47:191-201.
20. de Gregorio C, Estevez R, Cisneros R, Heilborn C, Cohenca N. Effect of EDTA, sonic, and ultrasonic activation on the penetration of sodium hypochlorite into simulated lateral canals: an in vitro study. *J Endod*. 2009;35:891-895.
21. Parente JM, Loushine RJ, Susin L, et al. Root canal debridement using manual dynamic agitation or the EndoVac for final irrigation in a closed system and an open system. *Int Endod J*. 2010;43:1001-1012.
22. Agarwal A, Deore RB, Rudagi K, Nanda Z, Baig MO, Fareez MA. Evaluation of apical vapor lock formation and comparative evaluation of its elimination using three different techniques: an in vitro study. *J Contemp Dent Pract*. 2017;18:790-794.
23. Vera J, Arias A, Romero M. Dynamic movement of intracanal gas bubbles during cleaning and shaping procedures: the effect of maintaining apical patency on their presence in the middle and cervical thirds of human root canals-an in vivo study. *J Endod*. 2012;38: 200-203.
24. Peeters HH, Gutknecht N. Efficacy of laser-driven irrigation versus ultrasonic in removing an airlock from the apical third of a narrow root canal. *Aust Endod J*. 2013;40:47-53.
25. Dioguardi M, Di Gioia G, Illuzzi G, et al. Passive ultrasonic irrigation efficacy in the vapor lock removal: systematic review and meta-analysis. *Sci World J*. 2019;1:8.
26. Schoeffel GJ. The EndoVac method of endodontic irrigation, part 2-efficacy. *Dent Today*. 2008;27:86-87.
27. Desai P, Himel V. Comparative safety of various intracanal irrigation systems. *J Endod*. 2009;35:545-549.
28. Magni E, Jäggi M, Eggmann F, Weiger R, Connert T. Apical pressures generated by several canal irrigation methods: a laboratory study in a maxillary central incisor with an open apex. *Int Endod J*. 2021;54:1937-1947.
29. de Gregorio C, Estevez R, Cisneros R, Paranjpe A, Cohenca N. Efficacy of different irrigation and activation systems on the penetration of sodium hypochlorite into simulated lateral canals and up to working length: an in vitro study. *J Endod*. 2010;36:1216-1221.
30. Gao Y, Haapasalo M, Shen Y, et al. Development and validation of a three-dimensional computational fluid dynamics model of root canal irrigation. *J Endod*. 2009;35:1282-1287.
31. Boutsioukis C, Verhaagen B, Versluis M, Kastrinakis E, van der Sluis LW. Irrigant flow in the root canal: experimental validation of an unsteady computational fluid dynamics model using high-speed imaging. *Int Endod J*. 2010;43:393-403.
32. Zhou N, Huang Z, Yu M, Deng S, Fu B, Jin H. Influence of needle working length and root canal curvature on irrigation: a computational fluid dynamics analysis based on a real tooth. *BMC Oral Health*. 2022;22(1):1-10.
33. Menter FR. Two-equation Eddy-viscosity turbulence models for engineering applications. *AIAA J*. 1994;32:1598-1605.
34. Duddridge JE, Kent CA, Laws JF. Effect of surface shear stress on the attachment of *Pseudomonas fluorescens* to stainless steel under defined flow conditions. *Biotechnol Bioeng*. 1982;24(1):153-164.
35. Yu M, Huang Z, Zhou N, Xu Z, Deng S, Jin H. Effect of inflow temperature on root canal irrigation: a computational fluid dynamics study. *Phys Fluids*. 2020;32(8):81903.
36. Kleier D, Averbach R, Mehdipour O. The sodium hypochlorite accident: experience of diplomates of the american board of endodontics. *J Endod*. 2008;34:1346-1350.
37. Guyton AC, Hall JE. *Textbook of Medical Physiology*. 11th ed. Elsevier; 2016.
38. Rito Pereira M, Silva G, Semiao V, et al. Experimental validation of a computational fluid dynamics model using micro-particle image velocimetry of the irrigation flow in confluent canals. *Int Endod J*. 2022;55:1394-1403.
39. Boutsioukis C, Lambrianidis T, Kastrinakis E, Bekiaroglou P. Measurement of pressure and flow rates during irrigation of a root canal ex vivo with three endodontic needles. *Int Endod J*. 2007;40:504-513.
40. Wang R, Shen Y, Ma J, et al. Evaluation of the effect of needle position on irrigant flow in the C-shaped root canal using a computational fluid dynamics model. *J Endod*. 2015;41:931-936.

41. Hu S, Duan L, Wan Q, Wang J. Evaluation of needle movement effect on root canal irrigation using a computational fluid dynamics model. *Biomed Eng Online*. 2019;18:52.
42. Park E, Shen Y, Khakpour M, Haapasalo M. Apical pressure and extent of irrigant flow beyond the needle tip during positive-pressure irrigation in an in vitro root canal model. *J Endod*. 2013;39:511-515.
43. Boutsioukis C, Gogos C, Verhaagen B, Versluis M, Kastrinakis E, van der Sluis LWM. The effect of root canal taper on the irrigant flow: evaluation using an unsteady computational fluid dynamics model. *Int Endod J*. 2010;43:909-916.
44. White FM. *Fluid Mechanics*. 4th ed. McGraw-Hill; 2017.

How to cite this article: Loroño G, Zaldívar JMR, Arias A, Dorado S, Jimenez-Octavio JR. Influence of needle design and irrigation depth in the presence of vapor lock: A computational fluid dynamics analysis in human oval roots with apical ramification. *Int J Numer Meth Biomed Engng*. 2023;e3742. doi:10.1002/cnm.3742